Available online at www.sciencedirect.com

SciVerse ScienceDirect

Ceramics International 39 (2013) 5407–5413

CERAMICS INTERNATIONAL

www.elsevier.com/locate/ceramint

Enhanced light scattering and photovoltaic performance for dye-sensitized solar cells by embedding submicron SiO_2/TiO_2 core/shell particles in photoanode

Yuanzhe Wang[a], Enlong Chen[a], Hongmei Lai[a], Bin Lu[b], Zhijuan Hu[a], Xiaomei Qin[a], Wangzhou Shi[a], Guoping Du[a,c,*]

[a]*Department of Physics, Shanghai Normal University, Shanghai 200234, P R. China*
[b]*College of Life and Environment Sciences, Shanghai Normal University, Shanghai 200234, P R. China*
[c]*School of Materials Science and Engineering, Nanchang University, Nanchang 330031, P R. China*

Received 14 September 2012; received in revised form 8 December 2012; accepted 13 December 2012
Available online 22 December 2012

Abstract

The introduction of light scattering in the photoanodes of dye-sensitized solar cells is one of the most effective approaches to enhance their photovoltaic performance. In this work, we prepared submicron SiO_2/TiO_2 core/shell particles and embedded these particles in the nanostructured TiO_2 photoanodes for light to scatter in the dye-sensitized solar cells. Due to the large difference in the refractive index between the SiO_2 core and the TiO_2 shell, the embedded submicron SiO_2/TiO_2 core/shell particles showed strong light scattering effect. Light absorbance of the dyed photoanode with the embedded SiO_2/TiO_2 particles for light scattering was found to be three times stronger than the one without light scattering particles over a wide wavelength range. The power conversion efficiency of dye-sensitized solar cells was increased by about 50% after the introduction of light scattering SiO_2/TiO_2 core/shell particles in the photoanode. This work will provide a base for further enhancement in the photovoltaic performance of dye-sensitized solar cells by optimizing the submicron SiO_2/TiO_2 core/shell particles and the photoanodes.

Keywords: Dye-sensitized solar cell; Light scattering; Core/shell particle; Nanostructure

1. Introduction

Due to its low manufacturing cost and potential high power conversion efficiency (PCE), dye-sensitized solar cell (DSSC) has been considered to be one of the most competitive photovoltaic devices in the future [1–4]. Compared with other types of solar cells, such as crystalline silicon solar cells, DSSC has its own unique advantages. The manufacturing process for DSSC is much simpler, and its impact on the environment during production is also relatively low. Nevertheless, at present, DSSC still has much lower PCE than that of the crystalline silicon solar cell.

In recent years, many research efforts have been made to enhance the PCE of DSSC. One of the most effective approaches to improve the photovoltaic performance of DSSC is to introduce a means of light scattering mechanism within the photoanode. A light scattering mechanism can significantly increase the optical traveling distance of sunlight within the photoanode so that the dyes have an opportunity to absorb more photons and consequently generate a greater number of free carriers for the DSSC. Thus, a DSSC equipped with such a light scattering mechanism will have a higher PCE.

Many techniques [5–12] have been employed to build light scattering mechanisms within the photoanodes for DSSCs, and large improvements in the PCE have been obtained. Liu et al. [7] prepared a trilayered photoanode for DSSC, where the top layer is composed of TiO_2 microflower particles and functions as a light scattering layer for the cell. In their work,

*Corresponding author at: Department of Physics, Shanghai Normal University, 100 Guilin Road, Shanghai 200234, P. R. China.
E-mail addresses: gpdu999@163.com, guopingdu@ncu.edu.cn (G. Du).

0272-8842/$ - see front matter © 2012 Elsevier Ltd and Techna Group S.r.l. All rights reserved.
http://dx.doi.org/10.1016/j.ceramint.2012.12.048

the short-circuit current density J_{sc} was enhanced by 60% over the cell without a light scattering layer. Fan et al. [8] fabricated a bilayered photoanode for DSSC, where the top and bottom layers were composed of TiO_2 nanorods (20–80 nm in diameter and 200–400 nm in length) and P25 TiO_2 nanoparticles. They found that the PCE of the DSSC increased by 66.5% via the light scattering layer. Yu et al. [9] fabricated DSSCs with bilayered photoanodes, in which the top layer intended for light scattering was composed of submicron TiO_2 particles with high porosity, while the bottom layer was built with TiO_2 nanoparticles. In their work, the PCE of DSSCs was found to increase from 6.92% to 9.04%. Dadgostar et al. [10] prepared hollow TiO_2 particles in the submicron scale and fabricated bilayered photoanodes for DSSCs, where the top layer for light scattering was composed of these hollow TiO_2 submicron particles. They observed a large enhancement in the PCE.

Due to its low cost and technical simplicity, the screen printing technique is generally employed to prepare the photoanode films for DSSCs. Preparation of the bilayer- or trilayer-structured photoanodes for light scattering in DSSCs usually requires two or three cycles of screen printing process. This will add on to the manufacturing cost for DSSCs, and is therefore not favored for mass production. It is desirable to prepare the photoanodes with light scattering capability in one step. Recently, Pham et al. [11] and Chou et al. [12] fabricated photoanodes with light scattering capability in one step. Pham et al. [11] prepared TiO_2 pastes by mixing TiO_2 nanoparticles, submicron polystryrene spheres (PS), and other additives, and then the paste was screen printed onto FTO glass. During sintering, the PS beads burnt out and were transformed into submicron cavities within the photoanode. These cavities were found to have strong scattering performance for the incoming sunlight. Besides an improvement in the photovoltaic performance for those DSSCs, another benefit is that the dye loading was also reduced by about 30%. Chou et al. [12] prepared TiO_2 pastes by mixing P25 TiO_2 nanoparticles, submicron TiO_2 particles, and other additives, and the paste was then used to fabricate the photoanodes in one step. These submicron TiO_2 particles acted as light scattering particles. They showed that the PCE was enhanced by a large amount.

In this work, we fabricated photoanodes with strong light scattering capabilities for DSSCs in one step. Instead of using cavities [11] or submicron TiO_2 particles [12] for light to scatter within the photoanode, we employed submicron SiO_2/TiO_2 core/shell particles, which were mixed with P25 TiO_2 nanoparticles to obtain the screen-printing paste for photoanode. In addition to the reduction of dye loading for DSSCs as shown by Pham et al. [11], the submicron SiO_2/TiO_2 core/shell particle should be more advantageous to the submicron cavities [11] and submicron TiO_2 particles [12] for light scattering in terms of the following two aspects:

1. The presence of submicron cavities within the photoanode of DSSC as in Ref. [11] can potentially deteriorate the mechanical stability of the photoanode. This can be harmful to the reliability of the DSSC devices. The use of submicron SiO_2/TiO_2 core/shell particles in this work should avoid such a reliability issue.
2. The submicron TiO_2 particles within the photoanode of DSSC as in Ref. [12] should have limited capability for light to scatter. This is because they have the same refractive index as that of the surrounding TiO_2 nanoparticles. According to the Mie Scattering theory [13], for a scattering particle, the larger the difference in refractive index between the scattering particle and the surrounding media, the greater the effective scattering area for the scattering particle. The refractive index of SiO_2 is about 1.46, while TiO_2 has a refractive index of about 2.56, much higher than the former. Thus, the submicron SiO_2/TiO_2 core/shell particles embedded within the photoandoe of DSSC should have a better performance in terms of light scattering than the TiO_2 particles.

Another point to be noted is that although the core SiO_2 is insulated, the shell TiO_2 can transport electrons generated by the adsorbed dyes. This work demonstrated that the photovoltaic performance of DSSC can be greatly enhanced by embedding submicron SiO_2/TiO_2 core/shell particles in the photoanode.

2. Experimental

2.1. Preparation of submicron SiO_2 particles

Submicron SiO_2 particles with different sizes were prepared using the modified Stöber method [14]. Ammonia, ethanol, and tetraethyl orthosilicate (TEOS) were of analytic purity. At first, ammonia with a concentration of 28%, ethanol, and deionized water in a volume ratio (9:16.25:24.75) were added into a breaker, and the 50 ml mixed solution was stirred at a speed of 1100 rpm for 5 min. In the meantime, we mixed 4.5 ml TEOS with 45.5 ml ethanol to obtain solution B. Solution B was then quickly poured into solution A which was stirred constantly at the speed of 1100 rpm. After stirring for 1 min, the stirring speed was reduced to 400 rpm. At that time the beaker was sealed with parafilm and left for two more hours for a complete reaction to obtain submicron SiO_2 particles. At last, the submicron SiO_2 particles were collected by a high-speed centrifugation at 8000 rpm, and washed with ethanol. This process was repeated three times before drying the submicron SiO_2 particles at 80 °C. The size of SiO_2 particles can be readily controlled by changing the mixing ratio of ammonia and deionized water in solution A.

2.2. Preparation of SiO_2/TiO_2 core/shell particles

The synthesis of SiO_2/TiO_2 core/shell particles was carried out as follows [15]: (1) 5 ml tetrabutyl titanate

(TBOT) was dissolved in 10 ml ethanol to obtain a mixed solution A; (2) 0.5 g as-prepared SiO_2 particles were dispersed in the solution A with the aid of ultrasonication for 10 min; (3) 20 ml ethanol and deionized water mixture (volume ratio = 5:1) were injected dropwise to solution A, and the mixture was kept stirring for 1 h; (4) the mixed solution was put into centrifuge tube and centrifuged for 10 min at the speed of 7000 rpm; (5) the products were collected and washed with ethanol; (6) steps (4) and (5) were repeated for three times and the mixed suspension was dried at 80 °C; and (7) the final products were collected and then calcined at 500 °C for 3 h to obtain the submicron SiO_2/TiO_2 core/shell particles.

2.3. Preparation of the photoanode for DSSC

The procedure to fabricate photoanodes for DSSCs with the submicron SiO_2/TiO_2 core/shell particles for light to scatter is as follows [16]. (1) P25 TiO_2 nanoparticles were dispersed in ethanol with the aid of ultrasonication for 30 min to obtain TiO_2 nanoparticle colloid. (2) The as-prepared submicron SiO_2/TiO_2 core/shell particles were added into the colloid and kept ultrasonicating for 30 min to obtain the hybrid colloid. The weight ratio of the P25 TiO_2 nanoparticles to the submicron SiO_2/TiO_2 core/shell particles was 90:10. (3) The hybrid colloid was put on a 60 °C hot plate with constant stirring until it became a thick paste. (4) Terpineol and ethyl cellulose were added to the above thick paste to obtain a screen-printing paste. (5) The paste was screen-printed onto the FTO-glass substrates, which had been soaked in the solution of 40 mM $TiCl_4$ at the temperature of 70 °C. The screen-printed substrates were then dried on a hotplate at 125 °C for 6 min. (6) After drying, the screen-printed substrates were then sintered in the following procedure, at 300 °C for 15 min, 400 °C for 20 min, and 500 °C for 30 min, and cooled down in the furnace to room temperature. The photoanodes were obtained, and their thickness was about 10 μm. (7) For dye loading, the photoanodes were immersed in the solution of N-719 dye (5×10^{-4} mol/L) for 24 h. (8) The dyed photoanodes were finally dried in N_2 atmosphere for the next day.

2.4. Assembling and characterization of DSSC

The counter electrode was obtained by depositing platinum (Pt) film on FTO-glass substrate via an electron beam evaporator. The width of two electrodes was adjusted to about 25 μm for embarking the liquid electrolyte. The space between electrodes was filled with a liquid electrolyte including 0.1 M LiI, 0.12 M I_2, 0.5 M 4-TBP and 1.0 M tetrabutylammonium iodide in acetonitrile from the opening of the sealing frame. A solar simulator (Class AAB, Abet 2000) providing an illumination of AM1.5G simulated sunlight and a Keithley 2440 source meter were employed to measure the photovoltaic properties of the assembled DSSC [17].

3. Results and discussion

3.1. Submicron SiO_2 particles

As reported previously, the size of submicron SiO_2 particles can be conveniently controlled by varying the ratio of ammonia to deionized water. Table 1 shows the different sizes (from 180 nm to 350 nm) for the submicron SiO_2 particles prepared in this work by using different amounts of ammonia and deionized water for the synthesis.

Fig. 1 shows the field emission scanning electron microscopy (FESEM, Hitachi S4800) images of the SiO_2 particles D3 (see Table 1). In agreement with the results reported by other researchers [14], these submicron SiO_2 particles, which were used as the cores to prepare SiO_2/TiO_2 core/shell particles, were of spherical shape and almost monodispersed. In addition, they were nonaggregated and their surfaces were smooth.

3.2. SiO_2/TiO_2 core/shell particles

The phase structures of the submicron SiO_2/TiO_2 core/shell particles were characterized using the X-ray diffraction technique (XRD, Bruker D8 Focus). Fig. 2 shows the XRD pattern of the submicron SiO_2/TiO_2 core/shell

Table 1
Submicron SiO_2 particles with different sizes.

	Chemicals used for synthesis			SiO_2
	Ammonia (ml)	Water (ml)	TEOS (ml)	diameter (nm)
D1	4.5	30	4.5	180
D2	4.5	18.5	4.5	240
D3	9	18.5	4.5	270
D4	9	24.75	4.5	300
D5	6.5	18.5	4.5	350

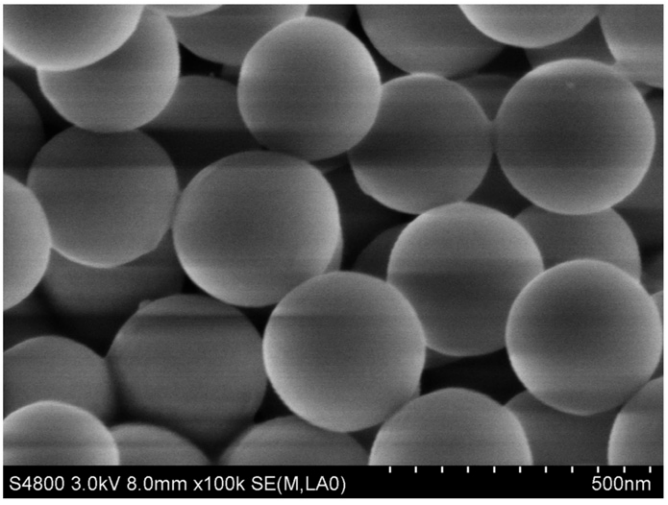

Fig. 1. FESEM image of the submicron SiO_2 particles (D3 in Table 1).

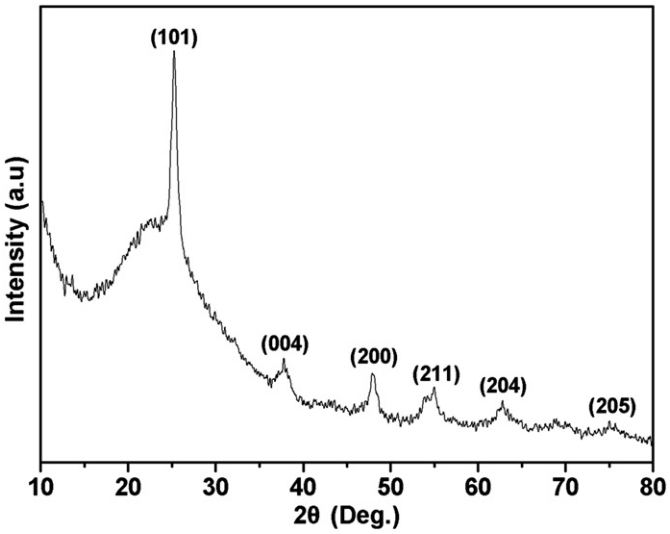

Fig. 2. XRD pattern of the SiO_2/TiO_2 core/shell particles. The diffraction peaks were indexed as the anatase TiO_2.

particles. All of the diffraction peaks in Fig. 2 can be readily indexed as the crystal planes of the anatase TiO_2 phase, while the diffuse peak located at 16–30° was attributed to the amorphous SiO_2.

The FESEM images in Fig. 3 show the morphologies of the SiO_2/TiO_2 core/shell particles, which are quite different from the cores as shown in Fig. 1. It is noted that the cores (see Fig. 1) were very smooth, while the shells (Fig. 3) were a bit rough and composed of TiO_2 nanoparticles. The existence of the core/shell structure can be better viewed on the particle as pointed by an arrow in Fig. 4a. It is noted in Fig. 4a that a small portion of the shell on the particle pointed by the arrow was peeled off, and the core was clearly exposed. The transmission electron microscopy (TEM, JEOL 2010) image in Fig. 4b also shows the morphologies of the submicron SiO_2/TiO_2 core/shell particles. It can be seen in Fig. 3 that the SiO_2/TiO_2 core/shell particles became larger than the core SiO_2 particles (see Table 1). It is noted that the SiO_2 core particles D1–D5 in

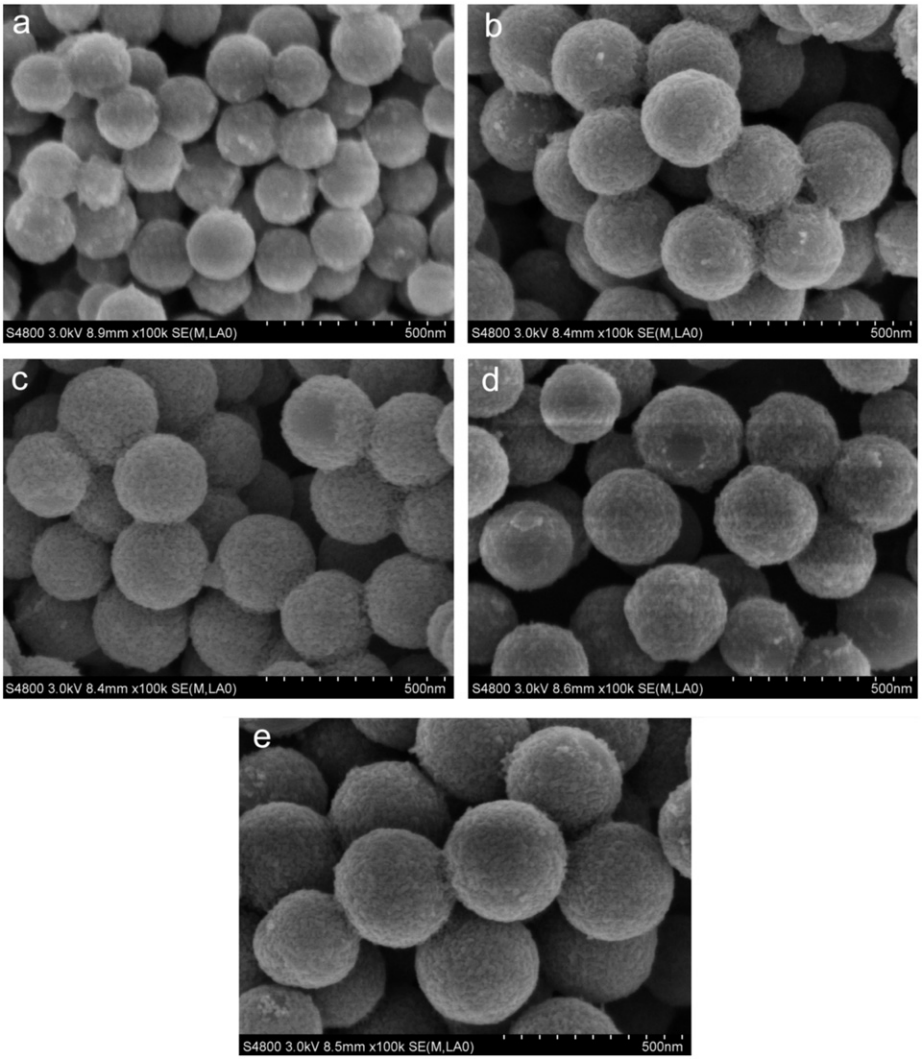

Fig. 3. FESEM images of the submicron SiO_2/TiO_2 core/shell particles. Particles in images a, b, c, d, and e are designed as W1, W2, W3, W4, and W5, respectively. W1–W5 correspond to D1–D5 in order in Table 1. The rough surface is the TiO_2 shell.

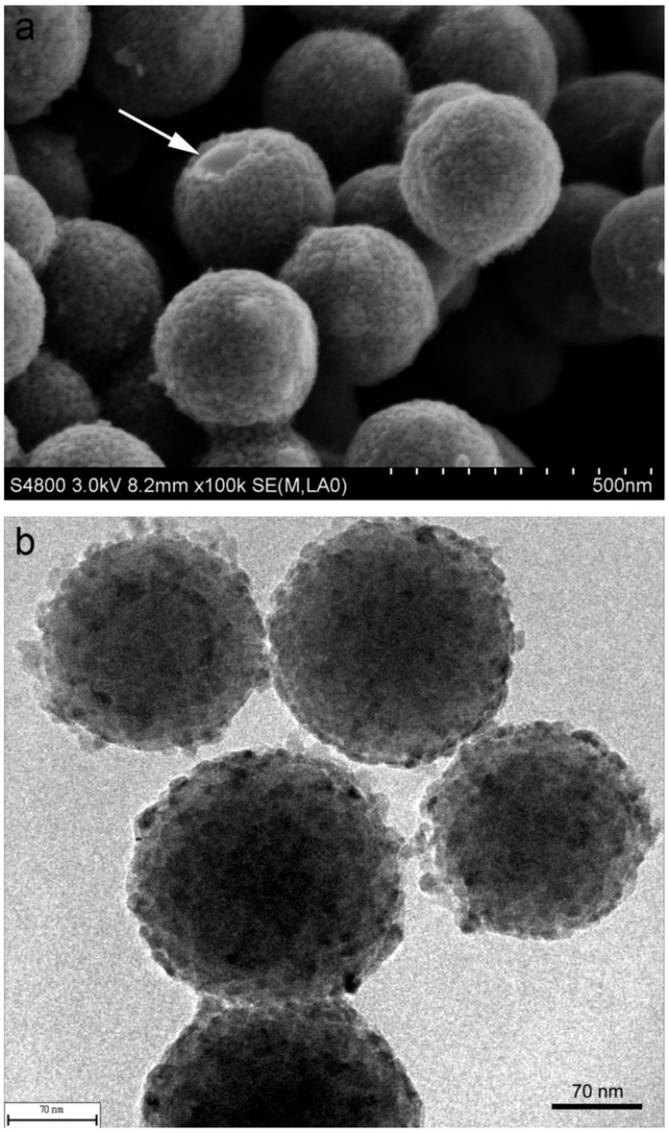

Fig. 4. FESEM (a) and TEM image (b) of the SiO_2/TiO_2 core/shell particles (W3). The particle pointed by the arrow was slightly peeled with the core exposed.

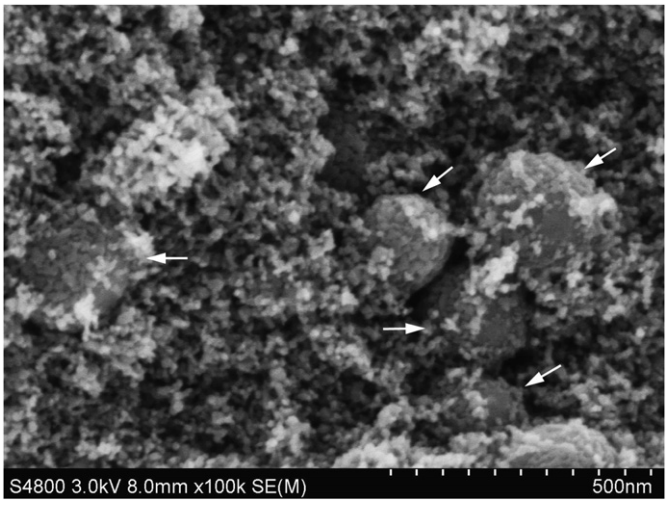

Fig. 5. FESEM image of the cross section of the photoanode with embedded SiO_2/TiO_2 core/shell particles (W3, marked with the white arrows).

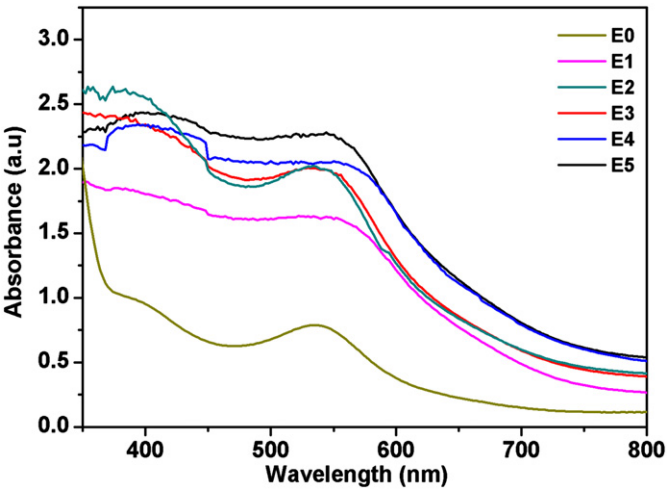

Fig. 6. Absorbance of the dyed photoanodes, E1–E5 with SiO_2/TiO_2 core/shell particles W1–W5 in order (see Fig. 3), E0 for reference with no light scattering particles.

Table 1 became the SiO_2/TiO_2 core/shell particles W1–W5 in sequence (Fig. 3). The sizes of the SiO_2/TiO_2 core/shell particles W1–W5 were about 200 nm, 260 nm, 300 nm, 320 nm, and 370 nm, in sequence. TiO_2 nanoparticles on the surfaces of the SiO_2 cores can be clearly seen in Fig. 4, and these shell TiO_2 nanoparticles had a diameter of about 20 nm.

3.3. Photoanodes and their optical properties

As stated in the Experimental Section 2.3, the submicron SiO_2/TiO_2 core/shell particles were embedded in the photoanode for light to scatter. The cross-section morphology of the photoanode was observed using FESEM after breaking it off. Fig. 5 shows the cross-section FESEM image of the photoanode with embedded submicron SiO_2/TiO_2 core/shell particles. As pointed by the white arrows in Fig. 5, the submicron SiO_2/TiO_2 core/shell particles were submerged within the surrounding TiO_2 nanoparticles, which had a size of about 20 nm. In addition to the strong light scattering by these submicron SiO_2/TiO_2 core/shell particles, the TiO_2 shell nanoparticles can also transport electrons inspite of the insulating SiO_2 cores. Thus, these submicron SiO_2/TiO_2 core/shell particles embedded in the photoanode should have similar electrical functionality to that of the submicron TiO_2 particles used in Ref. [12].

Photoanodes with embedded submicron SiO_2/TiO_2 core/shell particles W1–W5 of different sizes (see Section 3.2) were dyed for 24 h, and they were designated as photoanodes E1–E5, in sequence. For comparison, the reference photoanode without light scattering particles was named as E0. The optical absorbance of these dyed photoanodes

was then characterized. Fig. 6 shows the absorbance plots of these photoanodes E0–E5 over the wavelength range 350–800 nm. Photoanodes E1–E5 had much higher absorbance than that of E0 over the entire wavelength range. The absorbance peak at about 540 nm–550 nm was attributed to the fact that the N719 dye has the maximal optical absorption wavelength in this range [18]. It is noted in Fig. 6 that the absorbance of E5 in this wavelength range is over three times stronger than E0 over a wide wavelength range, implying a strong light scattering effect by the submicron SiO_2/TiO_2 core/shell particles.

Another characteristic in the absorbance plots (Fig. 6) for the photoanodes E1–E5 is that the absorbance generally increases with size of the submicron SiO_2/TiO_2 core/shell particles. This means that the submicron SiO_2/TiO_2 core/shell particles with the largest size (W5, about 370 nm in diameter) in this work showed the strongest light scattering performance. It is known that the smaller core/shell particles can adsorb relatively more dyes and therefore these core/shell particles may absorb more photons by themselves. However, the light scattering capability of the core/shell particles increases for a much higher value with their size. These larger core/shell particles therefore greatly lengthen the light traveling path within the photoanode so that much more photons can be absorbed by the dyes on their adjacent particles. This explains the results in Fig. 6.

3.4. Photovoltaic properties of DSSC

In this section, the DSSC cells fabricated from the photoanodes E0–E5 (see Section 3.3) were designated as S0–S5, in sequence. Table 2 shows the photovoltaic properties, including the open-circuit voltage V_{oc}, the short-circuit current density $_{sc}$, the fill factor *FF*, and the power conversion efficiency η of these solar cells S0–S5. The *J–V* curves for these DSSCs are shown in Fig. 7. It is obvious that these DSSCs (S1–S5) with light scattering particles had much higher η than that of the reference DSSC S0, which had no light scattering particles. DSSC S5 had the highest efficiency $\eta = 5.1\%$, while the reference DSSC S0 had an efficiency $\eta = 3.5\%$. This means that the submicron SiO_2/TiO_2 core/shell particles increased the efficiency of DSSC by about 50%. It is noted that the DSSCs showed higher η with the increase in the diameter of the core/shell SiO_2/TiO_2 light scattering particles. This result is generally in agreement with the optical absorbance data of these photoanodes (Fig. 6), suggesting that the light scattering effect from the submicron SiO_2/TiO_2 core/shell particles embedded in the photoanodes was responsible for the improvement in the photovoltaic properties of the DSSCs. It should be possible to further enhance the PCE of DSSC by optimizing the submicron SiO_2/TiO_2 core/shell particles and their concentration in the photoanode.

Table 2
J_{sc}, V_{oc}, *FF*, and η of the DSSCs.

Cell	J_{sc} (mA/cm^2)	V_{oc} (mV)	*FF* (%)	η (%)
S0	7.64	719.024	62.90	3.5 ± 0.02
S1	10.95	684.922	59.50	4.5 ± 0.02
S2	12.06	681.791	56.10	4.6 ± 0.01
S3	11.45	702.677	58.80	4.7 ± 0.02
S4	12.27	691.318	57.70	4.9 ± 0.01
S5	12.72	682.61	58.90	5.1 ± 0.02

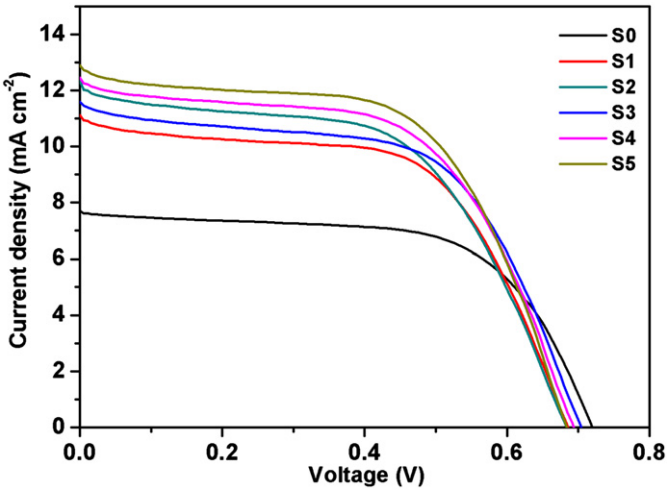

Fig. 7. *J–V* curves of the DSSCs. Cells S1–S5 had photoanodes E1–E5 in order (see Fig. 6), while cell S0 had photoanode E0.

4. Conclusions

We prepared submicron SiO_2/TiO_2 core/shell particles and embedded these particles in the nanostructured TiO_2 photoanodes for light to scatter in the dye-sensitized solar cells. The diameter of the core SiO_2 particles was from 180 nm to 350 nm, while the SiO_2/TiO_2 core/shell particles had a diameter from 200 nm to 370 nm. The embedded submicron SiO_2/TiO_2 core/shell particles showed strong light scattering effect, and the light absorbance of the dyed photoanode embedded with the SiO_2/TiO_2 light scattering particles was found to be three times stronger than the one without light scattering particles over a wide wavelength range. The power conversion efficiency of dye-sensitized solar cell was increased by about 50% after the introduction of light scattering SiO_2/TiO_2 core/shell particles in the photoanode. These results suggest that it is worthwhile to further optimize the submicron SiO_2/TiO_2 core/shell particles and their concentration in the photoanodes for the highest power conversion efficiency of dye-sensitized solar cells.

Acknowledgments

This work was supported by the Science and Technology Commission of Shanghai Municipality (10160503300), the R&D Project for Industrial Applications of Shanghai Normal University (DCL201104), the Leading Academic

Discipline Project of Shanghai Normal University (DZL804), the Innovation Program of Shanghai Municipal Education Commission (09YZ151), and the Program for Innovative Research Team (DXL902) of the Shanghai Normal University.

References

[1] B. O′Regan, M. Grätzel, A low-cost high-efficiency solar cell based on dye-sensitized colloidal TiO_2 films, Nature 353 (1991) 737–740.
[2] L.M. Gonçalves, V. de Zea Bermudez, H.A. Ribeiro, A.M. Mendes, Dye-sensitized solar cells: a safe bet for the future, Energy and Environmental Science 1 (2008) 655–667.
[3] M. Grätzel, Dye-sensitized solar cells, Journal of Photochemistry and Photobiology C 4 (2003) 145–153.
[4] M. Grätzel, Photoelectrochemical cells, Nature 414 (2001) 338–344.
[5] M. Grätzel, Recent advances in sensitized mesoscopic solar cells, Accounts of Chemical Research 42 (2009) 1788–1798.
[6] H.A. Atwater, A. Polman, Plasmonics for improved photovoltaic devices, Nature Materials 9 (2010) 205–213.
[7] M. Liu, H. Wang, C. Yan, G. Will, J. Bell, One-step synthesis of titanium oxide with trilayer structure for dye-sensitized solar cells, Applied Physics Letters 98 (2011) 133113.1–133113.3.
[8] K. Fan, W. Zhang, T. Peng, J. Chen, F. Yang, Application of TiO_2 fusiform nanorods for dye-sensitized solar cells with significantly improved efficiency, Journal of Physics Chemistry C 115 (2011) 17213–17219.
[9] I.G. Yu, Y.J. Kim, H.J. Kim, C. Lee, W.I. Lee, Size-dependent light-scattering effects of nanoporous TiO_2 spheres in dye-sensitized solar cells, Journal of Materials Chemistry 21 (2011) 532–538.
[10] S. Dadgostar, F. Tajabadi, N. Taghavinia, Mesoporous submicrometer TiO_2 hollow spheres as scatterers in dye-sensitized solar cells, ACS Applied Materials & Interfaces 4 (2012) 2964–2968.
[11] T.T.T. Pham, T. Bessho, N. Mathews, S.M. Zakeeruddin, Y.M. Lam, S. Mhaisalkar, M. Grätzel, Light scattering enhancement from submicron cavities in photoanode for dye-sensitized solar cells, Journal of Materials Chemistry 22 (2012) 16201–16204.
[12] C.S. Chou, M.G. Guo, K.H. Liu, Y.S. Chen, Preparation of TiO_2 particles and their applications in the light scattering layer of a dye-sensitized solar cell, Applied Energy 92 (2012) 224–233.
[13] H. Horvath, Gustav Mie and the scattering and absorption of light by particles: historic development and basics, Journal of Quantitative Spectroscopy and Radiative Transfer 110 (2009) 787–799.
[14] W. Stöber, A. Fink, E. Bohn, Controlled growth of monodesperse silica spheres in the micron size range, Journal of Colloid and Interface Science 26 (1968) 62–69.
[15] Z.H. Wang, L. Shen, S.Y. Zhu, Synthesis of core–shell Fe_3O_4@-SiO_2@TiO_2 microspheres and their application as recyclabe photocatalysts, Journal of Photoenergy (2012) 519–525.
[16] C.S. Chou, Y.J. Lin, R.Y. Yang, K.H. Liu, Preparation of TiO_2/NiO composite particles and their applications in dye-sensitized solar cells, Advanced Power Technology 22 (2011) 31–42.
[17] G.B. Wang, M.G. Fu, B. Lu, G.P. Du., L. Li, X.M. Qin, W.Z. Shi, Growth of nanocrystalline TiO_2 films by pulsed-laser-induced-liquid-deposition method and preliminary applications for dye-sensitized solar cells, Applied Physics A 100 (2010) 1169–1176.
[18] F.D. Angelis, S. Fantacci, E. Mosconi, M.K. Nazeeruddin, M. Grätzel, Absorption spectra and excited state energy levels of the N719 dye on TiO_2 in dye-sensitized solar cell models, Journal of Physical Chemistry C 115 (2011) 8825–8831.